Biweekly Periodic Deep Flow Variability on the Slope Inshore of the Kuril–Kamchatka Trench

KAZUYUKI UEHARA

Physical Oceanography Section, Mixed Water Region Fisheries Oceanography Division, Tohoku National Fisheries Research Institute, Shiogama, Miyagi, Japan

HIDEO MIYAKE

Laboratory of Physical Oceanography, Department of Fisheries Oceanography and Marine Science, Faculty of Fisheries, Hokkaido University, Hakodate, Hokkaido, Japan

26 July 1999 and 31 May 2000

ABSTRACT

Five long-term current records are analyzed to investigate the temporal variability for deep flows, from a single mooring fitted with two current meters on the slope inshore of the southern end of the Kuril–Kamchatka Trench southeast of Cape Erimo, where the Oyashio and a deep western boundary current are considered to flow southwestward together. At 3000 m the spectral peaks of eddy kinetic energy were found at about 2 weeks in all current records. The flow variability with period of 2 weeks at 3000 m was more energetic than that at 1000 m. By applying topographic Rossby wave theory, this variability is thought to be due to bottom-trapped topographic Rossby waves.

1. Introduction

Hallock and Teague (1996) pointed out that a deep western boundary current (DWBC) in the North Pacific basin flows southward along the continental slope inshore of the Japan Trench. Uehara and Miyake (1999, hereafter UM) also discussed the possibility of a southward DWBC along the slope inshore of the southern end of the Kuril–Kamchatka Trench from the existence of more energetic mean flows under the Oyashio in the analysis of data collected by direct current measurements at 41°30′N, 144°30′E, which is the same station discussed in this paper. Furthermore, they pointed out that the topographic β effect is not negligible in the steep bottom slope for deep flow variability of period less than 30 days.

In the North Atlantic, Thompson and Luyten (1976), Johns and Watts (1986), Pickart and Watts (1990), and many other scientists have reported that topographic Rossby waves (TRWs) are observed on the continental rise near Cape Hatteras in the region of a southward deep western boundary current, based on moored time series data. However, in the North Pacific, there are very few reports about TRWs in the DWBC region. In these regions, steep bottom slopes exist, such as the Japan Trench and the Kuril–Kamchatka Trench. It is considered that DWBCs are influenced significantly by the steep bottom slope leading to the trenches. In this paper, we investigate the biweekly periodic deep flow variability found from direct current measurements on the steep bottom slope inshore of the Kuril–Kamchatka Trench southeast of Cape Erimo, and then discuss the possibility of TRWs. This paper is the first attempt to detect TRWs in the region of a DWBC in the North Pacific.

2. Data

The mooring station named ER-2 (41°30′N, 144°30′E) is shown by the closed circle in Fig. 1. ER-2 is located on the steep bottom slope inshore of the sourthern end of the Kuril–Kamchatka Trench, where the water depth is about 3500 m and the direction of the local isobaths is roughly 220°T. The bottom topography near ER-2 along the cross-isobath direction is as sketched in Fig. 2. Bathymetric data were obtained from the routine hydrographic observation made by the Hakodate Marine Observatory (Oceanographic Observation Report 1997). In the vicinity of ER-2, the bottom slope is almost constant, about 4.8×10^{-2} (Fig. 2).

The mooring system installed at ER-2 was fitted with

Corresponding author address: Dr. Kazuyuki Uehara, Low Latitude Oceanography and Southern Resource Division, National Research Institute of Far Seas Fisheries, Shimizu, Shisuoka 424-8633, Japan.
E-mail: kuehara@enyo.affrc.go.jp

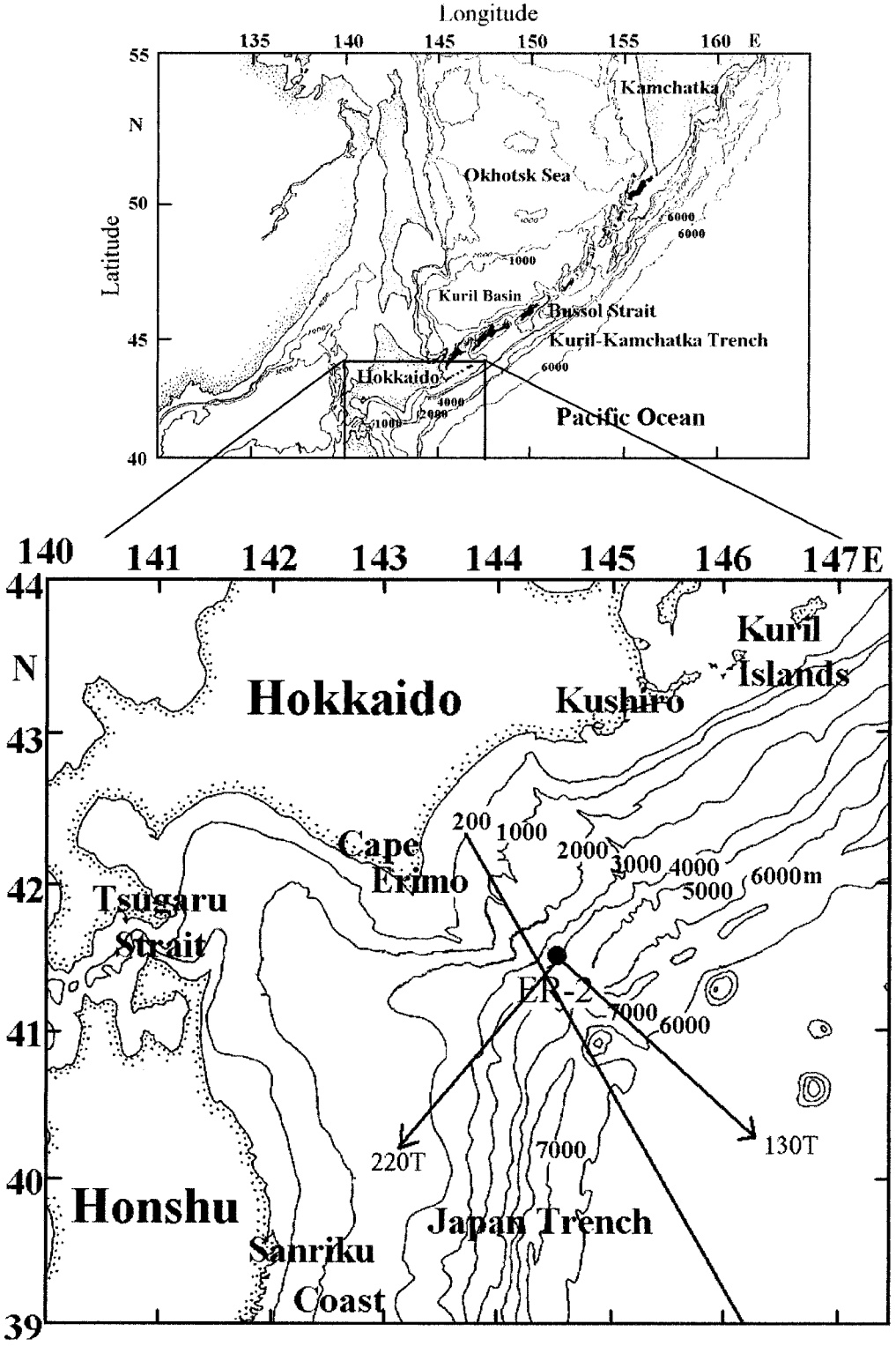

FIG. 1. Map showing the area in the vicinity of ER-2. The closed circles denote the mooring station ER-2. The arrows indicate the alongslope (220°T) and the downslope (130°T) directions. The solid line running from Cape Erimo to the southeast shows the line along the vertical bottom topography shown in Fig. 2.

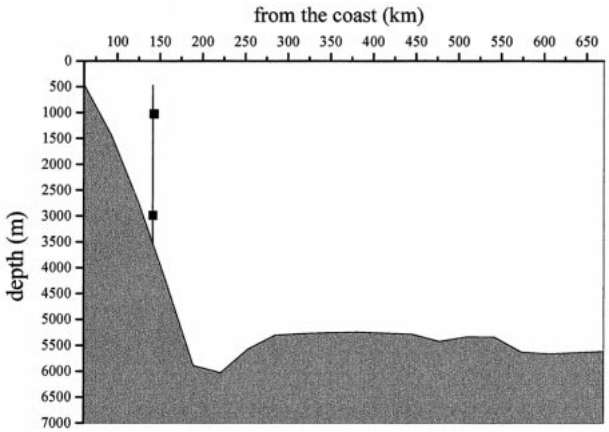

FIG. 2. Vertical bottom topography along the line shown in Fig. 1, and our mooring system at ER-2. Closed squares show the current meters moored in both the upper depth (1000 m) and the lower depth (3000 m).

TABLE 1. The period and instrument depths of current measurements at ER-2 off Cape Erimo.

Data name	Station	Depth (m)	Period	Data number
ER2-U-89	ER-2	1000	3 Jun 1989–9 Mar 1990	6726
ER2-L-89	ER-2	3000	3 Jun 1989–17 Mar 1990	6913
ER2-U-90	ER-2	1000	2 Jun 1990–17 Mar 1991	6946
ER2-L-90	ER-2	3000	2 Jun 1990–2 Apr 1991	7342
ER2-U-91	ER-2	1000	2 Jun 1991–3 Apr 1992	7363
ER2-L-91	ER-2	3000	2 Jun 1991–3 Apr 1992	7360
ER2-U-93	ER-2	1000	6 Apr 1993–10 Mar 1994	8166
ER2-L-93	ER-2	3000	6 Apr 1993–2 Feb 1994	7314
ER2-U-94	ER-2	1000	2 Jun 1994–2 Apr 1995	7298
ER2-L-94	ER-2	3000	2 Jun 1994–2 Apr 1995	7298

two current meters (Aanderaa, RCM-4) at nominal depths of 1000 m and 3000 m as illustrated in Fig. 2. The current measurements were conducted from June 1989 to March 1995. We then obtained five current records of 10–11 months duration each. Details of the observation periods are shown in Table 1. Time series of water temperature and current vectors obtained at 1-h intervals were smoothed by a low-pass Gaussian filter with an 81-h half-power point to remove high-frequency fluctuations such as tides and inertial oscillations. Daily mean velocity vectors and temperature were then derived. According to UM (Fig. 5 in their paper), the flow fluctuations at 3000 m are predominantly along the local isobaths in the direction of 220°T. We therefore decomposed the flow vectors into their alongslope component u (220°T) and the downslope component v (130°T), as shown in Fig. 1.

Routine hydrographic observations have been made by the Hakodate Marine Observatory four times a year at 20′ spatial intervals along the 41°30′N latitude from 141°40′E to 147°E. We use their CTD data to calculate the Brunt–Väisälä frequency (N) at 41°30′N, 145°00′E (Oceanographic Observation Report, 1989–95).

3. Biweekly periodic deep flow variability

To examine the flow variability, we computed frequency autospectra using the Blackman–Tukey method for the alongslope components u (220°T) and the downslope components v (130°T), removing the mean, windowing with a Hanning (cosine) window containing 10 degrees of freedom. The results are shown in Fig. 3. Confidence limits of 90% are shown in each figure.

At 1000 m, energy levels of spectra of u and v components are of similar magnitude at all frequency regions, and there are some spectral peaks in each observation period (Figs. 3a–e). However, specific spectral peaks for a common frequency in each observation period are not evident. On the other hand, at 3000 m spectral energies of u components are larger than those of v components for periods longer than about 10 days (Figs. 3f–j). These suggest that in the lower-frequency region the flow variability at 3000 m is predominant along local isobaths (220°T). Spectral peaks of u components at 13–15 days (biweekly; 0.077–0.066 cpd) occur during each observation period, as marked by downward arrows (Figs. 3f–j).

We focus on the biweekly variability apparent in the deeper current records by calculating bandpass filtered velocities, using a 2-day box filter with a 6-day half-power point and a 13-day box filter with a 27-day half-power point. Vector stick plots and temperature of the bandpassed series are shown in Fig. 4; the periodic flow reversals between 220°T and 40°T at 3000 m are clearly seen, and the amplitudes of the reversals are generally larger than those at 1000 m. Especially, for ER2-L-91 the amplitude of the periodic flow variability is clearly larger than that in ER2-U-91 (Fig. 4). Maxima of these values at 3000 m are about 5 cm s^{-1} or more. These biweekly periodic deep flows appear to fluctuate simultaneously with the shallow flows. This is supported by computing cross-spectra of the flows between 1000 and 3000 m as shown in Fig. 5. The biweekly deep flow variabilities found in the autospectra of u components have relatively high and significant values of coherence-squared functions, as marked by downward arrows, which exceed the 95% significance level (left panels in Fig. 5). The phases of the u components between 1000 and 3000 m at the biweekly periods are small values from about 2 to 42 h in all records (right panels in Fig. 5). In particular, it is seen that u components at 3000 m lead those at 1000 m in ER2-90, 91, and 93. In contrast, the coherence-squared values of v components at the biweekly periods are smaller than the 95% significance level, although we do not show this here. We can therefore conclude that the biweekly periodic deep flows are motions along the slope (220°T) and are coherent in the vertical direction over the depth range 1000 to 3000 m.

On the other hand, as shown in Fig. 4, amplitudes of the biweekly temperature variabilities at 3000 m are

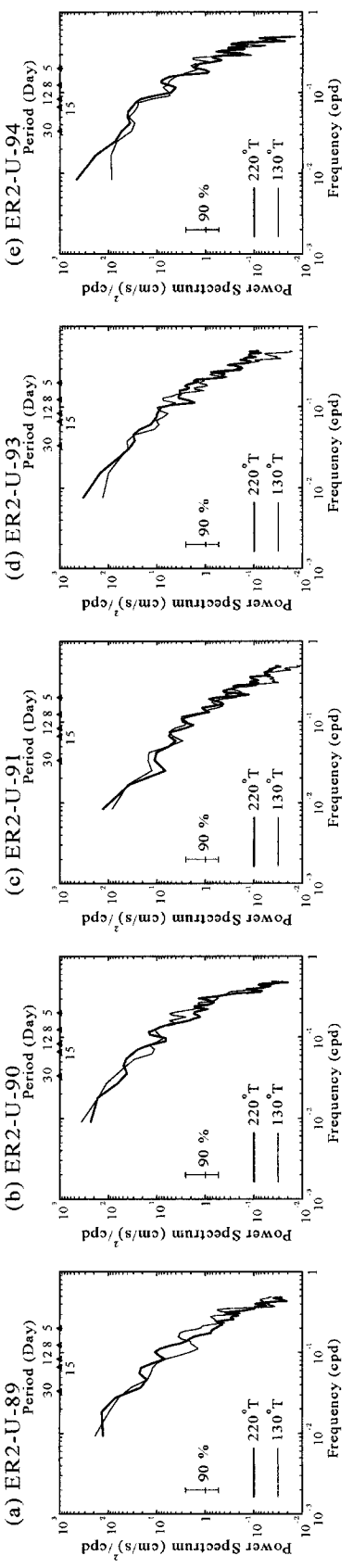

FIG. 3. Power spectral densities of the daily mean flows at ER-2 computed by the Blackman–Tukey method: (a) ER2-U-89, (b) ER2-U-90, (c) ER2-U-91, (d) ER2-U-93, (e) ER2-U-94, (f) ER2-L-89, (g) ER2-L-90, (h) ER2-L-91, (i) ER2-L-93, and (j) ER2-L-94. Solid thick lines and thin solid lines indicate the alongslope components (220°T) and downslope components (130°T), respectively. A vertical stick in each figure denotes a confidence limit of 90%. An arrow in each figure shows about 13–15 days period.

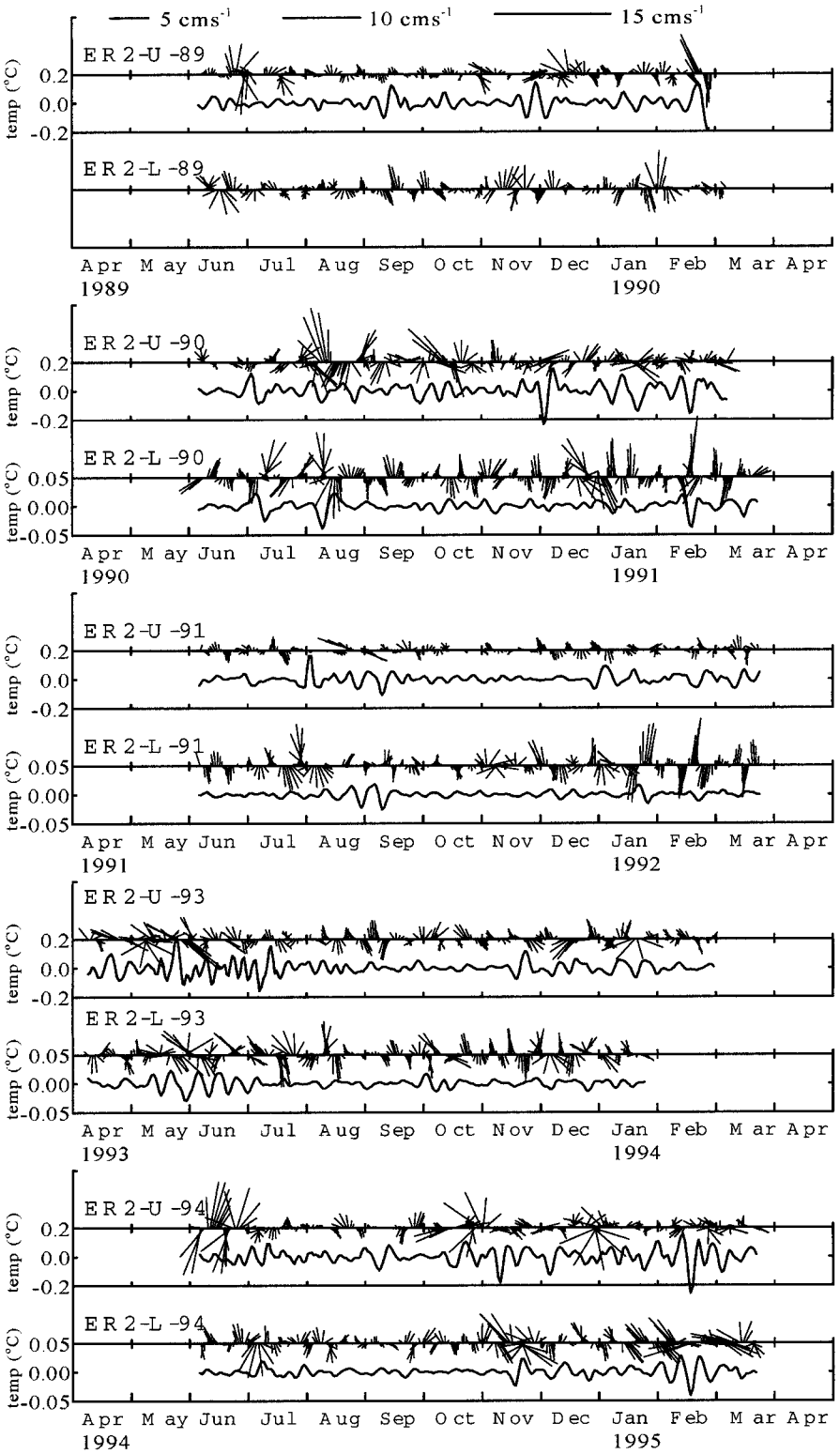

FIG. 4. Vector stick plots of the bandpassed flows at the center point of the 13-day period from ER-2. Notice that 220°T is up on these plots. Magnitude indicators of the flow vectors are shown on top of the figure.

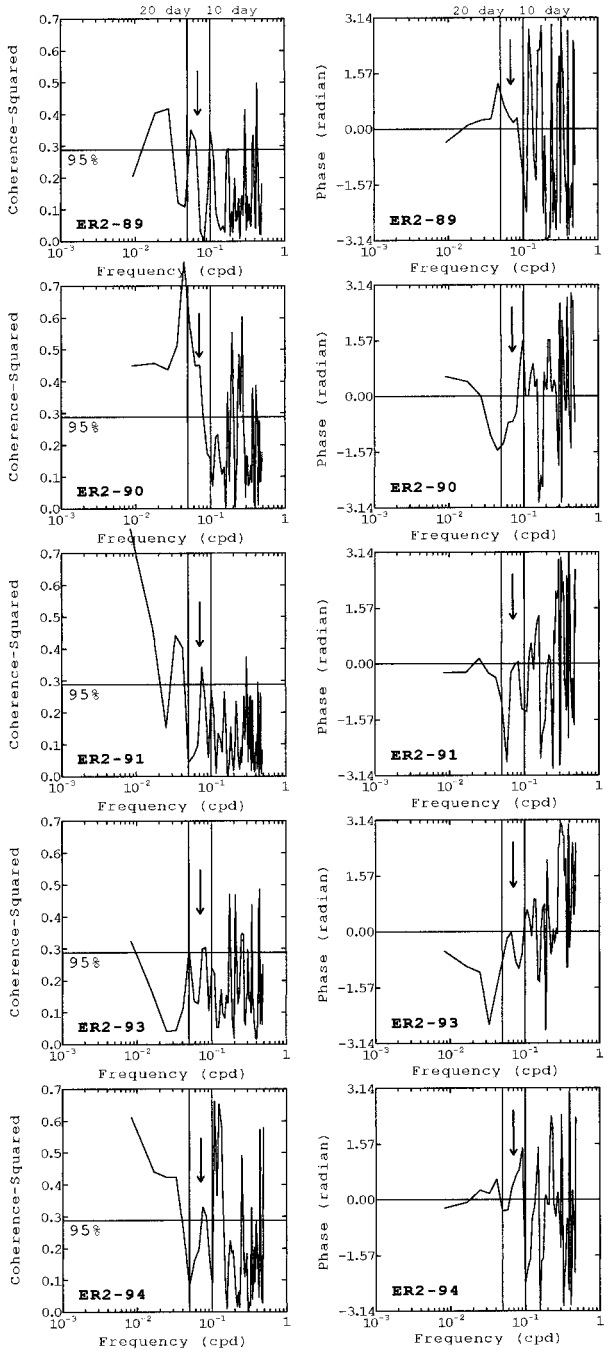

FIG. 5. Coherence-squared and phase functions of u components (220°T) between 1000 and 3000 m. Horizontal lines in coherence functions indicate the 95% confidence limit. An arrow in each bottom figure denotes the biweekly period as in Fig. 3. Two vertical lines in each figure show 20-day and 10-day periods, respectively.

quite small, less than ±0.005°C, whereas those at 1000 m show ±0.2°C or less. Johns and Watts (1986) reported that mean temperatures at about 3000-m depth near Cape Hatteras are 2.2°–3°C and their standard deviations are 0.066°–0.096°C. In Thompson and Luyten (1976), measured temperature also ranges from about 2.9 to about 3.3°C. However, temperature in our study area is quite low in itself, so its variability is also quite small. Temperature statistics of the daily mean flows are shown in Table 2. The mean values of temperature at 3000 m are 1.3°C and their standard deviations are 0.00°–0.03°C. These standard deviations are smaller than the current meter accuracy of ±0.05°C. We therefore cannot discuss temperature variability.

TABLE 2. Temperature statistics. $\overline{T}$ shows mean value over the entire series; ϵ, σ show the standard error and standard deviation, respectively. In ER2-L-89 statistics were not calculated because the temperature data are bad data in part.

Data name	$\overline{T}$ (°C)	ϵ	σ	Data number
ER2-U-89 (1000 m)	2.8	0.02	0.07	278
ER2-L-89 (3000 m)	—	—	—	286
ER2-U-90 (1000 m)	2.9	0.05	0.16	287
ER2-L-90 (3000 m)	1.3	0.01	0.03	303
ER2-U-91 (1000 m)	2.6	0.02	0.08	304
ER2-L-91 (3000 m)	1.3	0.00	0.01	304
ER2-U-93 (1000 m)	2.6	0.07	0.19	338
ER2-L-93 (3000 m)	1.3	0.01	0.03	302
ER2-U-94 (1000 m)	2.8	0.08	0.20	302
ER2-L-94 (3000 m)	1.3	0.00	0.02	302

From Figs. 4 and 5, the biweekly deep flow variabilities apparent in the deeper current records, which are coherent in the vertical direction, are considered to be bottom-trapped TRWs because their amplitudes decrease with increasing height off the bottom due to increased stratification. In the next section, we discuss the evidence supporting this hypothesis.

4. Topographic Rossby waves

In the vicinity of ER-2, the bottom topography is as sketched in Figs. 1 and 2. We assume that the bottom near ER-2 is a plane with southwest (220°T)–northeast (40°T) isobaths, with a constant downward slope of $\Gamma = 4.8 \times 10^{-2}$. The Brunt–Väisälä frequencies N at 41°30′N, 145°00′E near ER-2 were averaged over 5 years from 1989 to 1995, overlapping the periods of the current measurements, then were plotted in Fig. 6. We also assume that N is a constant because the variation of N in the vertical direction is very small below 1000 m. We choose $N = 10^{-3}$ (s^{-1}) as a reasonable value (Fig. 6). When the water depth is $H = 3500$ (m) and the Coriolis parameter is $f_0 = 10^{-4}$ (s^{-1}) at 41°30′N latitude, the value of topographic β becomes 1.4×10^{-9} (m^{-1} s^{-1}). This value is two orders of magnitude larger than planetary β of 1.7×10^{-11} at the same latitude. Therefore, we can neglect the planetary β effect. In this situation, a linear topographic Rossby wave model shows that the vertical structure of the bottom-intensified low-frequency wave motions is proportional to

$$V = V_0 \cosh\left(\frac{\kappa N}{f_0} z\right), \tag{1}$$

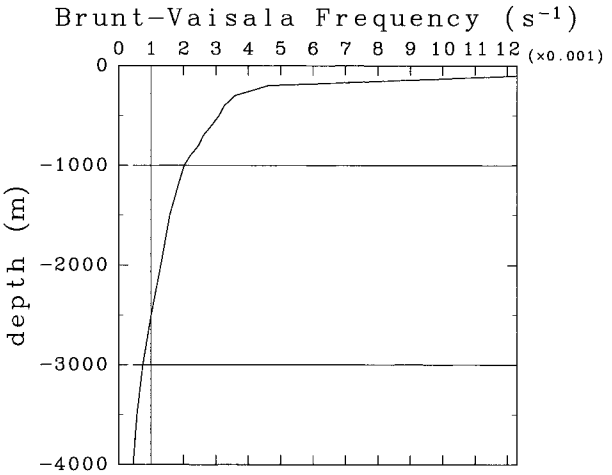

FIG. 6. Brunt–Väisälä frequency profile at 41°30′N, 145°E averaged over five years. Two horizontal lines denote the current meter depths at ER-2. The vertical line shows the value of 1.0×10^{-3} (s^{-1}).

where V is the horizontal velocity component, $\kappa = \sqrt{k^2 + l^2}$ is the horizontal wavenumber, and z is measured upward from $-H$ at the bottom (Rhines 1970). At this time, the dispersion relation for topographic Rossby waves in a stratified ocean neglecting planetary β can be written

$$\omega = \Gamma N \sin\theta \coth\left(\frac{\kappa H N}{f_0}\right), \tag{2}$$

where ω is frequency, and θ is the orientation angle of the wavenumber vector from downslope (Rhines 1970). From Eq. (1), we can therefore calculate the ratio of kinetic energy at the upper depth (z_1) to that at the lower depth (z_2), R, as follows:

$$R = \left(\frac{\cosh\left(\frac{\kappa N}{f_0} z_1\right)}{\cosh\left(\frac{\kappa N}{f_0} z_2\right)}\right)^2. \tag{3}$$

If topographic Rossby waves are observed, we obtain $R < 1$ at $|z_1| < |z_2|$. That is, kinetic energy at the lower depth is larger than that at the upper depth.

To estimate the wavenumber from Eq. (3), we computed the ratio of the spectra at 1000 m to those at 3000 m (Fig. 7). The ratios around the biweekly period for 220°T components are smaller than 1 in all observations (Fig. 7). That is, the kinetic energies of the biweekly flow variabilities at 3000 m are larger than those at 1000 m. On the other hand, for 130°T the ratios around the biweekly period are not smaller than 1, except for ER2-91 and ER2-93. Because the biweekly variabilities of the deep flow are predominant in the direction of 220°T and the ratios of the kinetic energy spectra of the biweekly variabilities along 220°T are smaller than 1 in all observations, we used the ratios of the 220°T com-

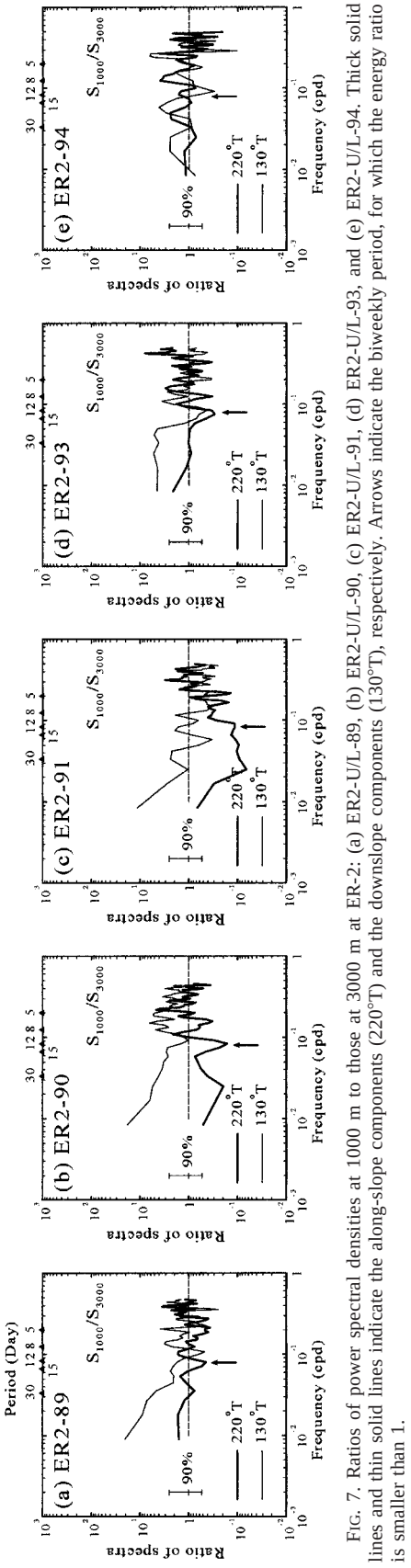

FIG. 7. Ratios of power spectral densities at 1000 m to those at 3000 m at ER-2: (a) ER2-U/L-89, (b) ER2-U/L-90, (c) ER2-U/L-91, (d) ER2-U/L-93, and (e) ER2-U/L-94. Thick solid lines and thin solid lines indicate the along-slope components (220°T) and the downslope components (130°T), respectively. Arrows indicate the biweekly period, for which the energy ratio is smaller than 1.

TABLE 3. Characteristics of the biweekly TRWs: R_{220} is the ratio of the spectra of u components at 1000 m to those at 3000 m, κ is the horizontal wavenumber derived from Eq. (3); λ is the wavelength. The phase speed, $C = \omega/\kappa$, is calculated from Eq. (2) and derived κ, and $\kappa NH/f_0$ indicates the stability parameter.

Data name	Period (day)	R_{220}	$\kappa NH/f_0$	λ (km)	κ (1 km^{-1})	C (km day^{-1})
ER2-89	14.0	0.55	1.01	217	0.029	16
ER2-90	13.3	0.23	1.75	126	0.050	9
ER2-91	13.3	0.13	2.21	100	0.063	8
ER2-93	13.3	0.30	1.47	146	0.043	11
ER2-94	15.0	0.89	0.42	506	0.012	34

ponent spectra for solving Eq. (3). Table 3 shows the ratios R, derived κ, the wave length (λ), the phase speed, $C = \omega/\kappa$, and the stability parameter, $\kappa NH/f_0$, for the biweekly period. Of course, ratios smaller than 1 exist for other than the biweekly periods. We discuss this in section 6.

Thompson and Luyten (1976) showed that principal axes of bandpassed current ellipses and wavenumber vectors are nearly perpendicular. To estimate the wavenumber vectors of the biweekly TRWs, we computed the direction of the principal major axis ϕ, which is measured anticlockwise from 220°T, as a function of frequency as follows (Fofonoff 1969):

$$\tan 2\phi = \frac{2K_{uv}}{S_u - S_v}, \tag{4}$$

where K_{uv} is the cospectrum of the u and v components, and S_u, S_v are the autospectra of the u, v components at 3000 m, respectively. The current ellipses of the biweekly period at 1000 and 3000 m are plotted in Fig. 8, which are based on the standard deviations along the principal major and minor axis components for the bandpassed flows. In addition, since the greatest horizontal velocity fluctuation is in the plane of the wave front, the estimated wavenumber vectors are also plotted, perpendicular to the ellipse orientations. Magnitudes of the vectors are based on spectral estimates. At 3000 m the bandpassed current ellipses are flattened close to the direction of the local isobaths (220°T, dashed lines in Fig. 8) and the magnitudes of the long axes (amplitudes are 1.3–2.2 cm s^{-1}) are larger than those at 1000 m in all cases (Fig. 8). Furthermore, the estimated wavenumber vectors deviate slightly from the downslope (130°T).

It is of interest to compare the direction of the wavenumber vectors estimated from our observations with those predicted from theory. From Eq. (2), we calculated the predicted orientation angles of the wavenumber vector, θ, as follows:

$$\theta = \sin^{-1}\left[\frac{2\pi}{T\Gamma N}\tanh\left(\frac{\kappa NH}{f_0}\right)\right], \tag{5}$$

using observed T (period), derived κ and other param-

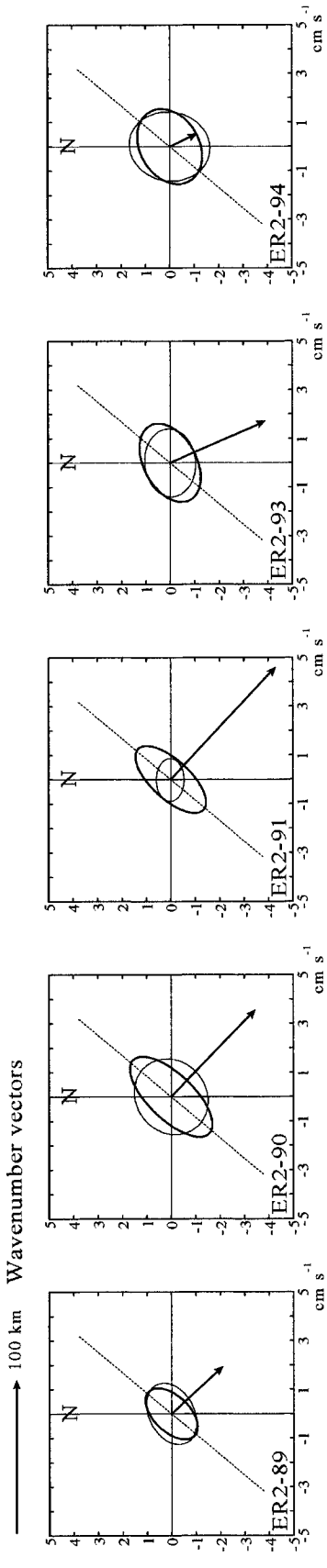

FIG. 8. The current ellipses of the biweekly period from ER-2 at 1000 m (thin ellipses) and the 3000 m (thick ellipses) in (a) ER2-89, (b) ER2-90, (c) ER2-91, (d) ER2-93, (e) ER2-94. These ellipses are plotted from the standard deviations of the principal major axis and minor axis of the band-pass filtered flow shown in Fig. 4. The arrow in each figure represents the estimated wavenumber vector with magnitude based on spectral estimates and direction perpendicular to the principal major axis of the bandpassed flows. Dashed lines indicate the direction of the local isobaths (220°T). Magnitude indicator of the wave lengths of 100 km is shown on top of the panels of ER2-89.

TABLE 4. Comparison of the orientation angles of the wavenumber vectors estimated from Eq. (4) and those predicted from Eq. (5). The estimated angles (ϕ_d) and θ is measured from downslope.

Data name	ϕ_d (deg)	θ (deg)
ER2-89	2	5.0
ER2-90	4	6.2
ER2-91	3	6.4
ER2-93	21	5.9
ER2-94	19	2.3

eters as mentioned previously. Table 4 shows the direction of the wavenumber vectors estimated from the principal major axes computed from Eq. (4) and those predicted from Eq. (5). Since θ is the orientation angle from downslope (130°T), the estimated orientation angles are measured in the same way (ϕ_d). The ϕ_d in ER2-89, ER2-90, and ER2-91 are in good agreement with theory (slightly smaller than θ). On the other hand, those in ER2-93 and ER2-94 are larger than theory, and not in such good agreement with theory (Table 4). However, when considering the uncertainty in determining the correct angle of the isobaths from Fig. 1 and the accuracy of flow directions measured by the current meters (±5°), these values are somewhat more reasonable. Therefore, the biweekly deep flow variability observed at ER-2 can be reasonably explained as bottom-trapped TRWs, propagating with the coast on the right hand and with the wave lengths (λ) and the phase speeds (C) listed in Table 3.

In ER2-94 the wavenumber κ is much smaller than that in the other cases, so the wave length is very large, 506 km (Table 3). Here the value of the stability parameter, $\kappa NH/f_0$, is less than 1; then $\cosh(\kappa NH/f_0) \approx 1$. Therefore, the vertical structure is almost uniform; that is, the motions in ER2-94 are considered to be more barotropic due to the long wave. In this case, stratification is not so important.

In contrast to the above, in ER2-90, ER2-91, and ER2-93 the wavelengths are on the order of 100–150 km (Table 3). Since these are $\kappa NH/f_0 > 1$, $\cosh(\kappa NH/f_0) > 1$. The horizontal velocities therefore decay rapidly upward from the bottom. In particular, in ER2-91 $\kappa NH/f_0$ has the large value of 2.21, so it is considered that the wave is more baroclinic due to its short wavelength. According to UM, the Oyashio extended to depths of 3000 m throughout the measurement period in ER2-91. This suggests a possibility that the TRW in ER2-91 is influenced by the vertical structure of the Oyashio.

5. Mean deep flows and biweekly TRWs

Uehara and Miyake reported that the deep flows (3000 m) at ER-2 are in part a deep western boundary current in the North Pacific basin from their analyses of energy statistics. We here discuss the biweekly TRWs in relation to the mean deep flows or the total fluctuating components. It is important to know ratios of kinetic energy of the biweekly TRWs to kinetic energy of the mean flows ($\overline{\text{KE}}$) or the total fluctuating components (eddy energy, KE′).

TABLE 5. The ratios of the biweekly kinetic energies of the bandpassed flows (KE_{TRW} in cm^2s^{-2}) to the kinetic energies of the mean deep flow ($\overline{\text{KE}}$ in cm^2s^{-2}) and the eddy kinetic energy (KE′ in cm^2s^{-2}). The values of $\overline{\text{KE}}$ and KE′ are quoted from Uehara and Miyake (1999).

Data name	KE_{TRW}	$\overline{\text{KE}}$	KE′	$\text{KE}_{\text{TRW}}/\overline{\text{KE}}$	$\text{KE}_{\text{TRW}}/\text{KE}'$
ER2-U-89 (1000 m)	1.34	0.34	10.52	3.93	0.07
ER2-L-89 (3000 m)	1.14	0.64	4.68	1.78	0.24
ER2-U-90 (1000 m)	2.40	1.00	18.16	2.40	0.13
ER2-L-90 (3000 m)	2.82	4.22	18.63	0.67	0.15
ER2-U-91 (1000 m)	0.58	9.39	5.04	0.06	0.12
ER2-L-91 (3000 m)	2.02	2.41	9.43	0.84	0.21
ER2-U-93 (1000 m)	1.56	8.68	12.04	0.18	0.13
ER2-L-93 (3000 m)	2.11	2.93	8.00	0.72	0.26
ER2-U-94 (1000 m)	2.44	2.13	15.82	1.15	0.15
ER2-L-94 (3000 m)	2.10	1.45	13.95	1.45	0.15

Table 5 shows the ratios of the kinetic energies of the bandpass filtered flows shown in Fig. 4 (KE_{TRW}) to $\overline{\text{KE}}$ and KE′. Here KE_{TRW} was calculated from the variance of the bandpassed flow; $\overline{\text{KE}}$ and KE′ were used from UM's results. In ER2-89 and ER2-94, KE_{TRW} at 3000 m are smaller than those at 1000 m. As shown in Fig. 8, this is because the current ellipses at 1000 m are more circular than those at 3000 m, although magnitudes of the alongslope components at 1000 m are smaller than those at 3000 m. We emphasize here that KE_{TRW} at 3000 m are almost the same magnitudes of about 2 $\text{cm}^2\ \text{s}^{-2}$, except for ER2-L-89, regardless of the magnitudes of $\overline{\text{KE}}$ (Table 5). According to UM's results, the intense mean deep flows are observed when their directions are southwestward along the local isobaths (ER2-L-90, -91, and -93). In contrast, when the mean deep flow has positive northward component (ER2-L-89) and is not along the local isobaths (ER2-L-94), it is weak. In ER2-L-90, 91, and 93, therefore, the ratios of KE_{TRW} to $\overline{\text{KE}}$ at the lower depth are smaller than 1; that is, the mean deep flows exceed the biweekly TRWs. On the other hand, in ER2-L-89 and 94 the ratios are larger than 1. In any case, even if the ratios are smaller than 1, the biweekly TRWs are comparable to the mean deep flows with ratios exceeding 0.60.

We find that the ratios of KE_{TRW} to KE′ are much smaller than 1 in all cases. That is, the biweekly TRWs are not predominant fluctuations relative to the total fluctuating components of the deep flows. We do not discuss this point here, but it is important to investigate what the predominant fluctuations are; further problems lie in this region.

6. The orientation angles of the wavenumber vector as a function of period

The ratios of the kinetic energies R [Eq. (3)], which are smaller than 1, are also found at other frequencies besides the biweekly period (Fig. 7). In particular, R in ER2-90 and ER2-91 are smaller than 1 in the lower-frequency regions (Figs. 7b,c). Therefore, we discuss here the relationships between the orientation angles from downslope computed from Eq. (5) and the angles of the principal major axis computed from Eq. (4) for all frequency regions at $R < 1$.

When κ is large, that is for short waves, $\tanh(\kappa NH/f_0)$ tends to 1, so Eq. (5) becomes

$$\theta_{\max} = \sin^{-1}\left(\frac{2\pi}{T\Gamma N}\right). \tag{6}$$

Equation (6) is an upper bound for the magnitude of θ. To compare the orientation angles of TRWs estimated from our observations with those predicted from theory, we plotted the angles measured from downslope resulting from Eq. (4), from Eq. (5), and upper bounds of the angles calculated from Eq. (6) as a function of period (day) in Fig. 9.

For all observations, in the higher frequency region (periods shorter than about 10 days) the observed angles vary widely as shown by open circles, and the changes in orientation of those versus period do not agree with those predicted from theory as shown by asterisks and crosses (Fig. 9). This suggests that the flow variabilities at 3000 m for short periods, which are larger in spectral energy than that at 1000 m, are not TRWs but some different motions. On the other hand, in the lower-frequency region (longer than about 10 days) the observed angles are close to the predicted ones, in comparison with those in the shorter periods. In particular, in ER2-90 and ER2-91, we can say that the changes in orientation of the observed angles roughly agree with those predicted, except for around 20 days period. These suggest the existence of long-term bottom trapped TRWs, longer than the biweekly period, with periods such as 40 and 120 days. However, in ER2-93 and ER-94, the observed angles are larger than the upper bounds for the longer periods. These angles disagree with predicted values even if we consider uncertainties in the observations and the spectral estimates. Pickart and Watts (1990) observed a 40-day TRW, which is in good agreement with theory, at Cape Hatteras within the DWBC in the western North Atlantic, using a moored array. They compared the change of the orientation angle of the principal axis as a function of period with that predicted from the dispersion relation [Eq. (2)]. Their result showed that the change of the observed angle is not in agreement with that of the predicted angle. They then explained these causes as the temporal variability of the DWBC itself and the upper-layer Gulf Stream. In our observations, it is considered that these disagreements between the observed and the predicted values are possibly due to the variability of the DWBC and the upper-layer Oyashio, but the cause is unknown. To clarify the cause, we need to observe widely in the horizontal direction, especially in the direction across the isobaths. Then the relation between the DWBC and the upper-layer Oyashio will be clarified, and we can find the variability of the DWBC itself if TRWs are clarified by observing widely in space.

7. Conclusions

We have investigated the periodic deep flow variability from five long-term current records on the steep bottom slope inshore of the Kuril–Kamchatka Trench southeast of Cape Erimo. From spectral estimates, we focused on the biweekly deep flow variabilities at 3000 m commonly found in all records. Their amplitudes are clearly larger than those at 1000 m. Moreover, these biweekly deep flow variabilities are predominant along the slope and coherent in the vertical direction. We therefore hypothesized that these deep motions, which are more energetic, are due to bottom trapped TRWs. We then estimated the wavenumber vectors based on the orientation angles of the principal major axis of the bandpassed current ellipses. We found that the orientations of estimated vectors in ER2-89, 90, 91 are in very good agreement with those predicted from theory. In ER2-93 and ER2-94 the two are not in such good agreement. However, when considering uncertainty in determining the correct angle of the isobath and the accuracy of the current meter, their estimated values are considered to be reasonable. We can therefore explain that the biweekly deep flow variabilities observed at ER-2 are due to bottom trapped TRWs.

Recently, mean horizontal deep circulations of the North Pacific have been gradually clarified by observing deep flows directly using mooring systems (Warren and Owens 1985, 1988; Hallock and Teague 1996; Uehara and Miyake 1999). However, we found that biweekly TRWs are comparable to the mean deep flows from energy statistics. In addition, these biweekly variabilities are less energetic than the total fluctuating components of the deep flows. Hence to understand the temporal variability of the DWBC itself, it is necessary for us take the effect of the TRWs into consideration first, when we observe DWBCs in the North Pacific.

Acknowledgments. We would like to thank the officers and crew of the T/S *Hokusei-maru*, Hokkaido University, who helped in the deployments and recoveries of the current meter moorings. We are grateful to Dr. Ito of Tohoku National Fisheries Research Institute for helpful discussions and suggestions. We also thank his colleagues, Drs. K. Okuda, O. Kato, and Mr. Y. Shimizu for their valuable discussions and comments. Thanks are extended to Hakodate Marine Observatory of Japan Meteorological Agency for supplying observational data. We are grateful to two anonymous reviewers for

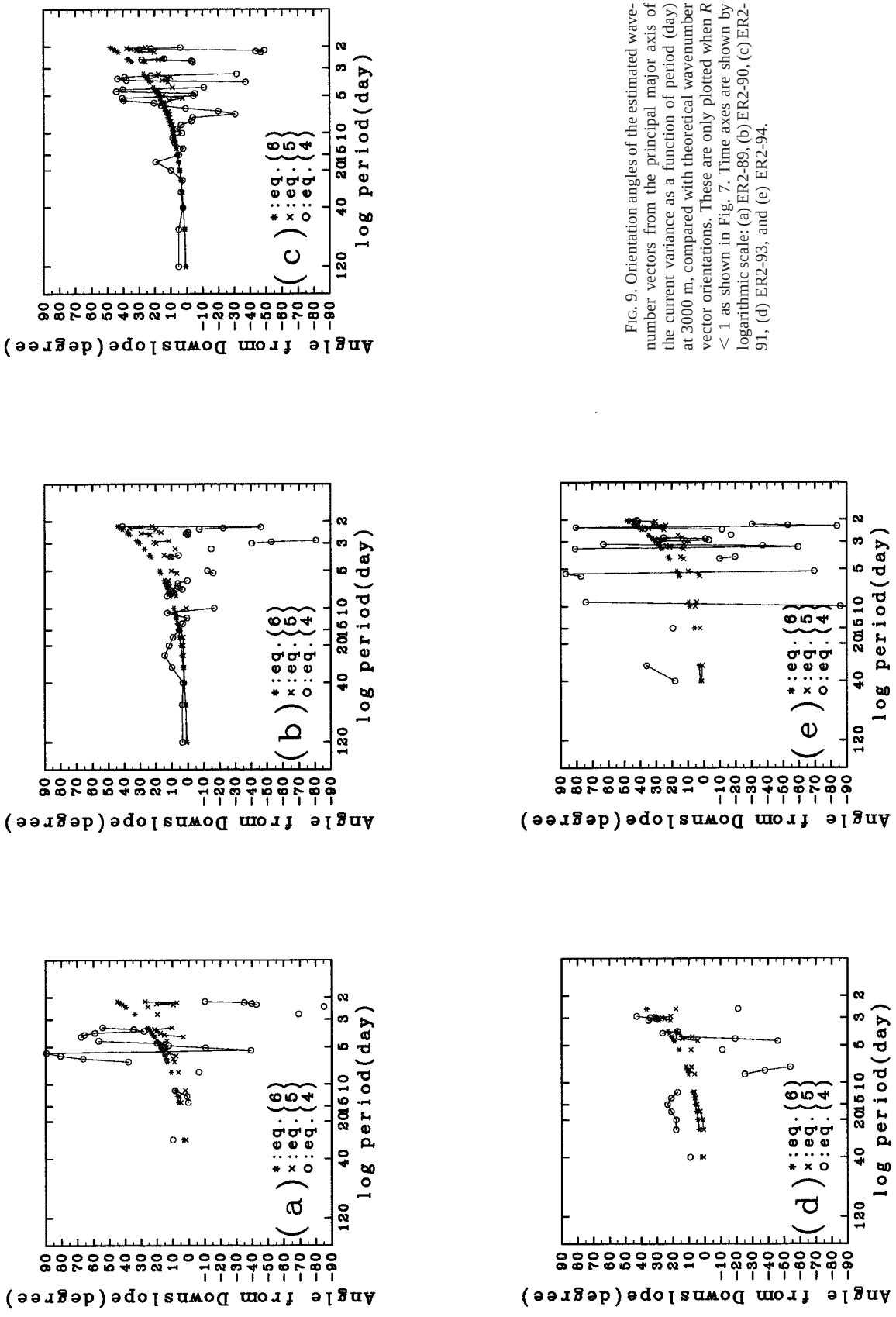

FIG. 9. Orientation angles of the estimated wavenumber vectors from the principal major axis of the current variance as a function of period (day) at 3000 m, compared with theoretical wavenumber vector orientations. These are only plotted when $R < 1$ as shown in Fig. 7. Time axes are shown by logarithmic scale: (a) ER2-89, (b) ER2-90, (c) ER2-91, (d) ER2-93, and (e) ER2-94.

their helpful suggestions and comments that improved the manuscript.

REFERENCES

Fofonoff, N. P., 1969: Spectral characteristics of internal waves in the ocean. *Deep-Sea Res.,* **16,** 59–71.

Hakodate Marine Observatory, 1989–1997: Oceanographic Observation Report (in Japanese with English figure and table captions). Vols. 27–35.

Hallock, Z. R., and W. J. Teague, 1996: Evidence for a North Pacific Deep Western Boundary Current. *J. Geophys. Res.,* **101,** 6617–6624.

Johns, W. E., and D. R. Watts, 1986: Time scales and structure of topographic Rossby waves and meanders in the deep Gulf Stream. *J. Mar. Res.,* **44,** 267–290.

Pickart, R. S., and D. R. Watts, 1990: Deep Western Boundary Current variability at Cape Hatteras. *J. Mar. Res.,* **48,** 765–791.

Rhines, P. D., 1970: Edge-, Bottom-, and Rossby Waves in a Rotating Stratified Fluid. *Geophys. Fluid Dyn.,* **1,** 273–302.

Thompson, R. O. R. Y., and J. R. Luyten, 1976: Evidence for bottom-trapped topographic Rossby waves from single moorings. *Deep-Sea Res.,* **23,** 629–635.

Uehara, K., and H. Miyake, 1999: Deep flows on the slope inshore of the Kuril–Kamchatka Trench southeast off Cape Erimo, Hokkaido. *J. Oceanogr.,* **55,** 559–573.

Warren, B. A., and W. B. Owens, 1985: Some preliminary results concerning deep northern boundary currents. *Progress in Oceanography,* Vol. 14, Pergamon, 537–551.

——, and ——, 1998: Deep currents in the central subartic Pacific Ocean. *J. Phys. Oceanogr.,* **18,** 529–551.